

## Fast rotation of an ultra-cold Bose gas

Vincent Bretin, Sabine Stock, Yannick Seurin, and Jean Dalibard  
 Laboratoire Kastler Brossel, 24 rue Lhomond, 75005 Paris, France  
 (Dated: July 18, 2003)

We study the rotation of a  $^{87}\text{Rb}$  Bose-Einstein condensate confined in a magnetic trap to which a focused, off-resonant gaussian laser beam is superimposed. The confining potential is well approximated by the sum of a quadratic and a quartic term which allows to increase the rotation frequency of the gas above the trap frequency. In this fast rotation regime we observe a dramatic change in the appearance of the quantum gas. The vortices which were easily detectable for a slower rotation become much less visible, and their surface density is well below the value expected for this rotation frequency domain. We discuss some possible tracks to account for this effect.

PACS numbers: 03.75.Lm, 32.80.Lg

The fast rotation of a macroscopic quantum object often involves a dramatic change of its properties. For rotating liquid  $^4\text{He}$ , superfluidity is expected to disappear for large rotation frequencies [1]. A similar effect occurs for type-II superconductors placed in a magnetic field, which lose their superconductivity when the field exceeds a critical value [2]. For the last few years it has been possible to set gaseous Bose-Einstein condensates into rotation, by nucleating in the gas quantized vortices which arrange themselves in a triangular lattice [3, 4, 5, 6, 7]. The theoretical investigation of the properties of these fast rotating gases has led to several possible scenarios. Depending on the confinement of the gas, its dimensionality and the strength of the interactions, theoretical predictions involve the nucleation of multiply charged vortices [8, 9, 10, 11], melting of the vortex lattice [12, 13], or effects closely connected to Quantum Hall physics [14, 15, 16, 17].

The confinement of cold atomic gases is generally provided by a magnetic trap which creates an isotropic transverse potential  $m \frac{1}{2} \omega_z^2 r_\perp^2$  in the plane perpendicular to the rotation axis  $z$  (we set  $x^2 + y^2 = r_\perp^2$ ). As the rotation frequency varies from 0 to  $\omega_z$ , the number of quantized vortices increases [18]. The limiting case of  $\omega = \omega_z$ , e.g. fast rotation, is singular: the confinement vanishes since the trapping force is compensated by the centrifugal force. In classical terms, the only remaining force on the particle is the Coriolis force. In quantum terms this corresponds to a gauge field  $A(r) = m \omega_z r^2$ . This is analog to the physics of charged particles in a uniform magnetic field and one expects to recover for weak interactions an energy spectrum with Landau levels separated by  $2\hbar\omega_z$ . However the absence of confinement in a pure harmonic trap rotating at  $\omega = \omega_z$  makes this study experimentally delicate [19]. The Boulder group recently reached  $\omega = 0.99\omega_z$  using evaporative spin-up [20].

In the present paper, following suggestions in [8, 9, 10, 11] we study the rotation of a Bose-Einstein condensate in a trap whose potential is well approximated by a superposition of a quadratic and a small quartic potential:

perposition of a quadratic and a small quartic potential:

$$V(r) = \frac{1}{2}m\omega_z^2 z^2 + \frac{1}{2}m\omega_z^2 r_\perp^2 + \frac{1}{4}kr_\perp^4 \quad (k > 0) : (1)$$

We can thus explore with no restriction the domain of rotation frequencies around  $\omega_z$ . Our results show a strong dependence of the behavior of the gas with  $\omega$ . For  $\omega = \omega_z < 0.95\omega_z$  we observe a regular vortex lattice. This lattice gets disordered when  $\omega$  increases. For  $\omega > \omega_z$  the number of detectable vortices is dramatically reduced although we have clear evidences that the gas is still ultra-cold and in fast rotation. We conclude this Letter by proposing some possible explanations for this behavior.

Our  $^{87}\text{Rb}$  condensate is formed by radio-frequency evaporation in a combined magnetic+laser trap. The pure magnetic trap provides a harmonic confinement along the 3 directions with the frequencies  $\omega_x^{(0)} = \omega_y^{(0)} = 75.5 \text{ Hz}$  and  $\omega_z = 11.0 \text{ Hz}$ . We superimpose a blue-detuned laser (wavelength 532 nm) propagating along the  $z$  direction to provide the quartic term in the confinement. The potential created by the laser is

$$U(r_\perp) = U_0 \exp\left(-\frac{2r_\perp^2}{w^2}\right) + U_0 \left[ \frac{2U_0}{w^2} r_\perp^2 + \frac{2U_0}{w^4} r_\perp^4 \right] : (2)$$

The laser's waist is  $w = 25 \mu\text{m}$  and its power is  $1.2 \text{ mW}$ . The first term  $U_0$  ( $k_B \approx 90 \text{ nK}$ ) in the right hand side of (2) is a mere shift of the energy scale. The second term is a correction of the transverse trapping frequency; we get for the combined magnetic-laser trap  $\omega_\perp = 65.6 \text{ Hz}$  [21]. The last term in (2) corresponds to the desired quartic confinement, with  $k = 2.6(3) \cdot 10^{11} \text{ J m}^{-4}$ . The expansion in (2) is valid for  $r_\perp \ll w$ , which is indeed the case for all data presented here.

We start the experimental sequence with a quasi-pure condensate that we stir using an additional laser beam, also propagating along  $z$  [4]. This laser stirrer creates an anisotropic potential in the  $xy$  plane which rotates at a frequency  $\omega_{\text{stir}}$ . To bring the condensate in rotation at a frequency close to  $\omega_z$ , we use two stirring phases. First

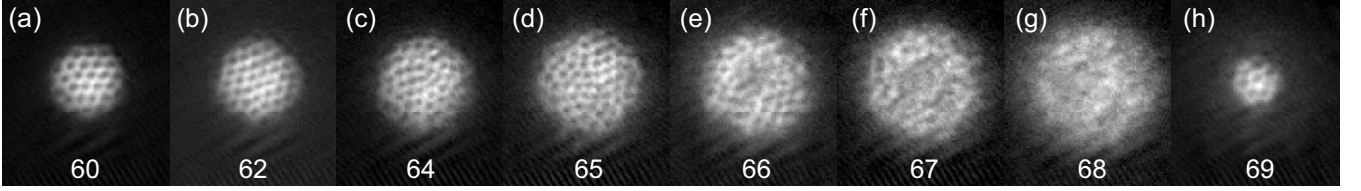


FIG. 1: Pictures of the rotating gas taken along the rotation axis after 18 ms time of flight. We indicate in each picture the stirring frequency  $\omega_{\text{stir}}^{(2)}$  during the second stirring phase ( $\omega_{\text{stir}}^{(1)} = 65.6$  Hz). The real vertical size of each image is 306  $\mu\text{m}$ .

we choose  $\omega_{\text{stir}}^{(1)}, \omega_{\text{stir}}^{(2)} = \frac{p}{2}$ , so that the stirring laser resonantly excites the transverse quadrupole mode  $m = +2$  of the condensate at rest [22]. The duration of this first excitation is 300 ms and we then let the condensate relax for 400 ms in the axisymmetric trap. This procedure sets the condensate in rotation, with a vortex lattice containing typically 15 vortices.

We then apply the laser stirrer for a second time period, now at a rotation frequency  $\omega_{\text{stir}}^{(2)}$  close to or even above  $\omega_{\text{c}}$ . For the condensate with 15 vortices prepared during the first phase, the transverse quadrupole mode is shifted to a higher frequency and can now be resonantly excited by a stirrer rotating at  $\omega_{\text{stir}}^{(2)} \approx \omega_{\text{c}}$  [7, 23]. The second stirring phase lasts for 600 ms. It is followed by a 500 ms period during which we let the condensate equilibrate again in the axisymmetric trap. At this stage the number of trapped atoms is  $3 \times 10^6$ .

We find that this double nucleation procedure is a reliable way to produce large vortex arrays and to reach effective rotation frequencies  $\omega_{\text{e}}$  around or above  $\omega_{\text{c}}$ . In particular it is much more efficient than the procedure which consists in applying permanently the stirring laser while increasing continuously its frequency. It has one drawback however: the effective rotation frequency  $\omega_{\text{e}}$  of the gas after equilibration might differ significantly from the rotation frequency  $\omega_{\text{stir}}^{(2)}$  that we apply during the second stirring phase. The role of the stirring phase is to inject angular momentum in the system, and the rotation frequency of the atom cloud may subsequently change if the atom distribution (hence the moment of inertia) evolves during the final equilibration phase.

The rotating atom cloud is then probed destructively by switching off the confining potential, letting the cloud expand during  $t_{\text{exp}} = 18$  ms and performing absorption imaging. We take simultaneously two images of the atom cloud after time of flight (TOF). One imaging beam is parallel to the rotation axis  $z$  and the other one is perpendicular to  $z$  [24].

Fig. 1a-h show a series of images taken along the  $z$  axis and obtained for various  $\omega_{\text{stir}}^{(2)}$  around  $\omega_{\text{c}}$ . When  $\omega_{\text{stir}}^{(2)}$  increases, the increasing centrifugal potential weakens the transverse confinement. This leads to an increasing radius in the  $xy$  plane. As it can be seen from the transverse and longitudinal density profiles of Fig. 2, obtained for

$\omega_{\text{stir}}^{(2)} = 66$  Hz, the gas after TOF has the shape of a pancake. The limit of our method for setting the gas in fast rotation is shown on the image (h) at the extreme right of Fig. 1. It corresponds to  $\omega_{\text{stir}}^{(2)} = 69$  Hz, far from the quadrupole resonance of the condensate after the first nucleation. In this case we could not bring the gas in the desired fast rotation regime.

For the pictures (e,f) obtained with  $\omega_{\text{stir}}^{(2)} = 66$  and 67 Hz, the optical thickness of the cloud has a local minimum in the center; this indicates that the confining potential in the rotating frame,  $V_{\text{rot}}(r) = V(r) - \frac{1}{2} \omega_{\text{e}}^2 r^2$ , has a Mexican hat shape. The effective rotation frequency  $\omega_{\text{e}}$  thus exceeds  $\omega_{\text{c}}$ . The striking feature of these images is the small number of visible vortices which seems to conflict with a large value of  $\omega_{\text{e}}$ . The main goal of the remaining part of this Letter is to provide more information on this puzzling regime.

In order to analyze quantitatively the pictures of Fig. 1, we need to model the evolution of the cloud during TOF. For a pure harmonic potential ( $k = 0$ ), a generalization of the analysis of [25] to the case of a rotating condensate shows that the expansion in the  $xy$  plane is well described by a scaling of the initial distribution by the factor  $(1 + \frac{1}{2} \omega_{\text{e}}^2 t^2)^{1/2}$  [26]. We assume here that this is still approximately the case for a condensate prepared in a trap with a non zero quartic term  $k r^4/4$ .

We have analyzed a series of 60 images such as those of Fig. 1, assuming an initial atomic distribution given by the Thomas-Fermi law:

$$n(r) = \frac{m}{4\pi^2 a^3} \left( 1 - \frac{V_{\text{rot}}(r)}{V_0} \right); \quad (3)$$

where  $a = 5.2$  nm is the scattering length characterizing the atomic interactions and  $V_0$  the chemical potential. The optical thickness for the imaging beam propagating along  $z$ , proportional to the column atomic density in the  $xy$  plane, varies as  $(1 + \frac{1}{2} \omega_{\text{e}}^2 t^2)^{3/2}$ , where  $\omega_{\text{e}}$  can be expressed in terms of the physical parameters of the problem [27]. An example of the  $t$ , which takes  $\omega_{\text{e}}$  as adjustable parameters, is given in Fig. 2a. The agreement is correct, though not as good as for condensates confined in purely harmonic traps. This may be a consequence of the approximate character of the scaling transform that we use to describe the TOF evolution. The resulting values for  $\omega_{\text{e}}$  as a function of  $\omega_{\text{stir}}^{(2)}$  are

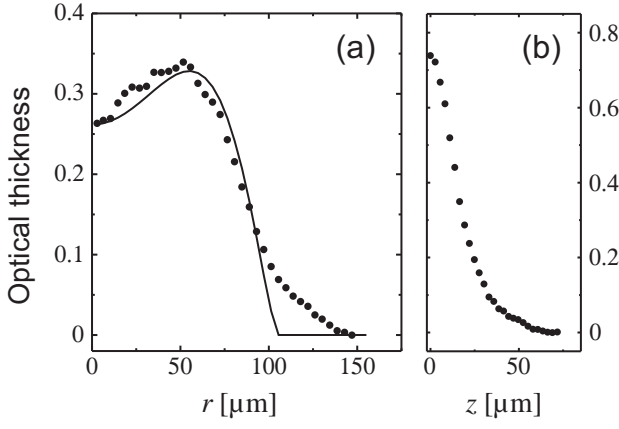


FIG. 2: Optical thickness of the atom cloud after time-of-flight for  $\Omega_{\text{stir}}^{(2)} = 66$  Hz. (a) Radial distribution in the xy plane of Fig. 1e. Continuous line: fitting the Thomas-Fermi distribution (3). (b) Distribution along the z axis averaged over  $|x| < 20$   $\mu\text{m}$  (imaging beam propagating along y).

given in Fig. 3. We find  $\Omega_{\text{stir}}^{(2)}$  for stirring frequencies  $\Omega_{\text{stir}}^{(2)} = 68$  Hz. Note that for  $\Omega_{\text{stir}}^{(2)} = 68$  Hz (image Fig. 1g) the quality of the fit is comparatively poor due to local inhomogeneities of the atom cloud.

From the value of  $\Omega_{\text{stir}}^{(2)}$  given by the fit, we recover the atom number  $N$ . For the largest measured rotation frequency, the Thomas-Fermi distribution (3) corresponds to a nearly spherical atom cloud before TOF (diameter 29  $\mu\text{m}$  in the xy plane and length 34  $\mu\text{m}$  along z).

A second determination of the effective rotation frequency  $\Omega_{\text{eff}}$  of the condensate is provided by the vortex surface density after TOF. Assuming that the vortex pattern is scaled by the same factor as the condensate density, we deduce the vortex density  $\nu_v$  before TOF, hence the rotation frequency  $\Omega_{\text{eff}} = \nu_v / m$  [18]. For  $\Omega_{\text{stir}}^{(2)} < \Omega_{\text{c}}^{(2)}$ , the value of  $\Omega_{\text{eff}}$  deduced in this way and plotted in Fig. 3 is in fair agreement with the one deduced from the fit of the images. On the contrary, for  $\Omega_{\text{stir}}^{(2)} = 66$ –68 Hz the number of distinguishable vortices is much too low to account for the rotation frequencies determined from the fits of the TOF images.

In order to gather more information on the rotational properties of the gas, we now study the two transverse quadrupole modes  $m = \pm 2$  of the gas. We recall that these two modes have the same frequency for a non-rotating gas, due to symmetry. For a rotating gas in the hydrodynamic regime, the frequency difference  $\Omega_{+2} - \Omega_{-2}$  is proportional to the ratio between the average angular momentum of the gas and its moment of inertia, which is nothing but the desired effective rotation frequency  $\Omega_{\text{eff}}$  [23]. The strength of this approach is that it does not make any assumption on the expansion during TOF.

To study these transverse quadrupole modes, we briefly illuminate the rotating gas using the laser stirrer, now with fixed axes [28]. This excites a superposition of the

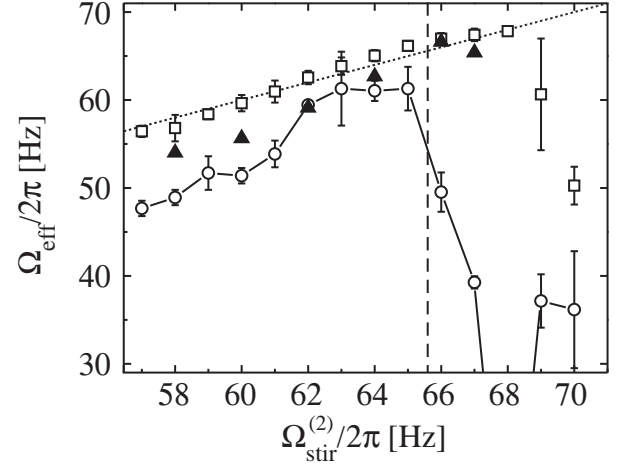


FIG. 3: Effective rotation frequency  $\Omega_{\text{eff}}$  as a function of the stirring frequency  $\Omega_{\text{stir}}^{(2)}$ .  $\circ$ : values deduced from the fit using the Thomas-Fermi distribution (3).  $\square$ : values obtained by measuring the vortex density in the TOF pictures.  $\triangle$ : values obtained using surface wave spectroscopy. The bars indicate standard deviations.

modes  $m = \pm 2$  with equal amplitudes. We then let the cloud evolve freely in the trap for an adjustable duration and we perform the TOF analysis. From the time variation of both the ellipticity of the cloud in the xy plane and the inclination of its eigenaxes, we deduce  $\Omega_{\text{eff}}$ , hence the effective rotation frequency  $\Omega_{\text{eff}} = (\Omega_{+2} - \Omega_{-2})/2$ . The corresponding results are plotted in Fig. 3. They are in good agreement with the results obtained from the fits of the images:  $\Omega_{\text{eff}} \approx \Omega_{\text{stir}}^{(2)}$ . Consequently they conflict with the rotation frequency that one derives from the vortex surface density when  $\Omega_{\text{stir}}^{(2)} = 66$ –68 Hz.

To explain the absence of visible vortices in the regime  $\Omega_{\text{stir}}^{(2)} = 66$ –68 Hz, one could argue that the gas might be relatively hot, hence described by classical physics. The equilibrium state should then correspond to rigid body rotation. However all experiments shown here are performed in presence of radio-frequency (rf) evaporative cooling. The rf is set 24 kHz above the value which empties the trap and it eliminates all atoms crossing the horizontal plane located at a distance  $x_{\text{ev}} = 19$   $\mu\text{m}$  below the center (one-dimensional evaporation). From evaporative cooling theory [29, 30] we know that the equilibrium temperature  $T$  of the rotating gas is a fraction of the evaporation threshold  $V_{\text{rot}}(x_{\text{ev}}) = 32$  nK for  $\Omega_{\text{eff}} = 67$  Hz [31]. This indicates that  $T$  is in the range of 5–15 nK, well below the critical temperature at this density (180 nK for an estimated density  $3 \times 10^3$   $\text{cm}^{-3}$ ) [32]. This low temperature is also confirmed by the small decay rates of the quadrupole modes ( $\sim 20$   $\text{s}^{-1}$ ), characteristic of  $T \ll T_c$ .

The estimated temperature  $T$  is of the order of the splitting between Landau levels  $2\pi\hbar^2 k_B^{-1} = 6.3$  nK, so

that only the first two or three levels are appreciably populated. For each Landau level, the rf evaporation eliminates states with an angular momentum  $L_z = \hbar m$  ( $\omega_{ev} = a_{ho}^2 / 200$ , where  $a_{ho} = \hbar / (m \omega_{ho})$  is the ground state's size of the harmonic oscillator with frequency  $\omega_{ho}$ ).

A first possibility to interpret our data consists in assuming that the whole gas shown in Fig. 1e-g is rotating, that it is in the degenerate regime, and that it cannot be described by a single macroscopic wave function since the number of distinguishable vortices is too low to account for the measured rotation frequency. In this point of view, the state of the system is therefore more complex than a single Hartree state. A theoretical analysis along this line, involving the formation of composite bosons, has been very recently proposed in [34].

A second possible explanation is that the vortices are still present for  $\omega_{ho} > \omega_{ev}$ , but that the vortex lines are strongly tilted or bent, so that they do not appear as clear density dips in the images of Fig. 1e-g. This could be for example a consequence of the residual anisotropy of the trapping potential in the xy plane [21]. In an experiment performed at  $\omega_{ho} = 0.95 \omega_{ev}$ , the Boulder group has shown that a static anisotropy of 4% reduces considerably the vortex visibility over a time scale of 0.8 s [33]. However the residual anisotropy of our trap is  $< 1\%$  and this effect should be limited, unless the vortex lattice becomes notably more fragile as  $\omega_{ho}$  approaches  $\omega_{ev}$ . The distortion of the vortex lattice could also result from a strong increase of the crystallization time for  $\omega_{ho} > \omega_{ev}$  which would then exceed the 500 ms equilibration time  $\tau_{eq}$ . To check this effect, we have increased  $\tau_{eq}$  up to 2 s without noticing any qualitative change in the atom distribution (for larger  $\tau_{eq}$  the gas slows down significantly).

A third possibility is that a small fraction of the gas has stopped rotating during the standard 500 ms equilibration time, and can therefore be at a higher temperature [32]. This small fraction could decrease the visibility of the vortices present in the condensed part of the cloud. The existence of such a fraction could be tested by a quantitative analysis of the density profiles of Fig. 2ab. Such an analysis should take into account the TOF evolution of an interacting atomic cloud initially confined in a non harmonic potential.

To summarize we have presented in this Letter a direct evidence for a qualitative change in the nature of a degenerate Bose gas when it is rotated around and above the trapping frequency. We plan to complement this study by an analysis of other modes of the rotating gas, such as the transverse breathing mode [35]. Several other interesting phenomena have been predicted and remain to be investigated experimentally for this type of potential: existence of several phases involving either a vortex array with a hole, or a giant vortex [8, 9, 10, 11, 13]. Another extension of the present work consists in transposing the experimental scheme to a 2D geometry, where the motion along z would be frozen. The situation would then be the

bosonic analog of the situation leading to the quantum Hall effect, provided the effective rotation frequency of the gas is precisely adjusted to the trap frequency.

We thank P. Rosenbusch for participation in earlier stages of this experiment, and S. Stringari, L. Pitaevskii, G. Baym and the ENS group for useful discussions. This work is partially supported by CNRS, College de France, Region Ile de France, DAAD, DGA, DRED and EU (CQG network HPRN-CT-2000-00125).

- 
- [\*] Unité de Recherche de l'Ecole normale supérieure et de l'Université Pierre et Marie Curie, associée au CNRS.
- [1] R.J. Donnelly, Quantized Vortices in Helium II, (Cambridge, 1991), Chaps. 4 and 5.
  - [2] M. Tinkham, Introduction to superconductivity (McGraw-Hill, 1996).
  - [3] M.R. Matthews et al., Phys. Rev. Lett. 83, 2498 (1999).
  - [4] K.W. Madison et al., Phys. Rev. Lett. 84, 806, (2000).
  - [5] J.R. Abo-Shaeer et al., Science 292, 476 (2001).
  - [6] E. Hodby et al., Phys. Rev. Lett. 86, 2196 (2001).
  - [7] P.C. Haljan et al., Phys. Rev. Lett. 87, 210403 (2001)
  - [8] A.L. Fetter, Phys. Rev. A 64, 063608 (2001).
  - [9] E. Lundh, Phys. Rev. A 65, 043604 (2002).
  - [10] K. Kasamatsu et al., Phys. Rev. A 66, 053606 (2002)
  - [11] G.M. Kavoulakis and G. Baym, New Jour. Phys. 5, 51.1 (2003).
  - [12] J. Sinova et al., Phys. Rev. Lett. 89, 030403 (2002)
  - [13] U.R. Fisher and G. Baym, Phys. Rev. Lett. 90, 140402 (2003).
  - [14] N.R. Cooper et al., Phys. Rev. Lett. 87, 120405 (2001).
  - [15] B. Paredes et al., Phys. Rev. Lett. 87, 010402 (2001).
  - [16] T.-L. Ho, Phys. Rev. Lett. 87, 060403 (2001).
  - [17] N. Regnault and Th. Jolicœur, Phys. Rev. Lett. 91, 030402 (2003).
  - [18] C. Raman et al., Phys. Rev. Lett. 87, 210402 (2001).
  - [19] P. Rosenbusch et al., Phys. Rev. Lett. 88, 250403 (2001).
  - [20] P. Engels et al., Phys. Rev. Lett. 90, 170405 (2003).
  - [21] We measure an oscillation frequency of 65.4 (3) Hz along the vertical axis x and 65.9 (3) Hz along the horizontal axis y.
  - [22] K.W. Madison et al., Phys. Rev. Lett. 86, 4443 (2001).
  - [23] F. Zambelli and S. Stringari, Phys. Rev. Lett. 81, 1754 (1998); M. Cozzini and S. Stringari, Phys. Rev. A 67, 041602 (R) (2003).
  - [24] P. Rosenbusch et al., Phys. Rev. Lett. 89, 200403 (2002).
  - [25] Y. Castin and R. Dum, Phys. Rev. Lett. 77, 5315 (1996).
  - [26] F. Chevy, PhD thesis (Paris, 2001).
  - [27] Such a simple formula could not be obtained for the column density along y, hence the absence of a fitting function in Fig. 2b.
  - [28] F. Chevy et al., Phys. Rev. Lett. 85, 2223 (2000).
  - [29] W. Ketterle and N. Van Druten, Advances in Atomic, Molecular, and Optical Physics, 37, 181 (1996).
  - [30] O. Luiten, M. Reynolds, and J. Walraven, Phys. Rev. A 53, 381 (1996).
  - [31] For a precise evaluation of the evaporation threshold, one must keep the gaussian variation of  $U(r_z)$  in Eq. (2) rather than using its quadratic+quartic approximation.
  - [32] The rotation of the gas is crucial for establishing a link

between the evaporation radius and the temperature. For a gas at rest, the evaporation threshold is  $V(x_{ev})$  instead of  $V_{rot}(x_{ev})$ , which corresponds to a much higher temperature (100-200 nK).

[33] P. Engels et al, Phys. Rev. Lett. 89, 100403 (2002).

[34] E. Akkermans and S. Ghosh, cond-mat/0307418.

[35] S. Stock, V. Bretin, and J. Dalibard, to be published.